PAIN®

VIDEO · OPEN

Peripheral nerve injury results in a biased loss of sensory neuron subpopulations

Andrew H. Cooper[a], Allison M. Barry[b], Paschalina Chrysostomidou[a], Romane Lolignier[a], Jinyi Wang[a], Magdalena Redondo Canales[a], Heather F. Titterton[a], David L. Bennett[b], Greg A. Weir[a],*

Abstract

There is a rich literature describing the loss of dorsal root ganglion (DRG) neurons following peripheral axotomy, but the vulnerability of discrete subpopulations has not yet been characterised. Furthermore, the extent or even presence of neuron loss following injury has recently been challenged. In this study, we have used a range of transgenic recombinase driver mouse lines to genetically label molecularly defined subpopulations of DRG neurons and track their survival following traumatic nerve injury. We find that spared nerve injury leads to a marked loss of cells containing DRG volume and a concomitant loss of small-diameter DRG neurons. Neuron loss occurs unequally across subpopulations and is particularly prevalent in nonpeptidergic nociceptors, marked by expression of Mrgprd. We show that this subpopulation is almost entirely lost following spared nerve injury and severely depleted (by roughly 50%) following sciatic nerve crush. Finally, we used an in vitro model of DRG neuron survival to demonstrate that nonpeptidergic nociceptor loss is likely dependent on the absence of neurotrophic support. Together, these results profile the extent to which DRG neuron subpopulations can survive axotomy, with implications for our understanding of nerve injury–induced plasticity and pain.

Keywords: Sensory neuron, Neuron death, Transgenic reporter line, Neuropathic pain, Nerve injury

1. Introduction

Dorsal root ganglion (DRG) neurons represent a molecularly and functionally heterogeneous population. Under normal conditions, this diversity contributes to the ability of the somatosensory nervous system to detect a myriad of sensory stimuli that result in the perceptions of touch, temperature, itch, and pain. Following nerve injury, physiological changes in DRG neurons lead to hyperexcitability,[57] which is a key pathological driver of neuropathic pain.[20,63] Concomitant molecular changes in discrete subpopulations also occur, and these have recently been comprehensively described in single-cell[37,44] and subpopulation-specific sequencing studies.[3] These studies describe a transient and generalized reduction in the expression of subpopulation-specific genes following nerve injury.[3,37,44]

In addition to molecular changes, there is a rich literature describing the frank loss of DRG neurons following traumatic nerve injury in experimental rodent models.[24,50,53,56] Some studies have suggested that neuron loss occurs in certain patient cohorts,[48,66] but this is yet to be definitively demonstrated in humans. In rodents, most studies support a preferential loss of small cells that give rise to unmyelinated fibers[53] but some contrasting studies describe the preferential loss of large cells[6] or loss of cells of all sizes.[46] Variation is evident across studies in terms of experimental species, age, type of injury, and quantification methods.[56] Shi et al.[50] used stereological counting methods to identify a 54% loss of DRG neuron number 4 weeks after "mid-thigh" sciatic nerve transection in C57BL/6 mice. Estimates for the degree of loss following commonly used nerve injury paradigms (eg, spared nerve injury [SNI] and sciatic nerve crush) are not available and because of the neurochemical changes following injury and the loss of subpopulation marker gene expression,[5,44,50] the vulnerability of molecularly defined subpopulations has not been characterized. Moreover, more recent studies have cast doubt on the extent or even presence of DRG neuron death following nerve injury. One study which developed a deep learning approach to assess rat DRG cellular plasticity found no loss of neurons up to 2 weeks post-SNI,[49] while another observed no loss of genetically labelled damaged DRG neurons 2 months after sciatic nerve crush.[44]

The issue of whether neuron loss occurs, and if so, in what subpopulations, is important. It will likely have implications for our understanding of reinnervation and functional recovery in patients. Furthermore, better insight will provide critical context for those investigating the plasticity that occurs following nerve injury and may inform therapeutic targeting of sensory neuron populations.

An expanding repertoire of transgenic recombinase driver lines now makes it possible to permanently label DRG neuron subpopulations and study their fate in rodent nerve injury paradigms. The aim of this study was to use this technology to characterize

neuron loss after nerve injury and to test the hypothesis that loss is not equally distributed across molecular populations.

2. Methods

2.1. Animals

Mice were housed in groups in humidity- and temperature-controlled rooms with free access to food and water, on a 12-hour light–dark cycle, and with environmental enrichment. Animal procedures were performed under a UK Home Office Project Licence and in accordance with the UK Home Office (Scientific Procedures) Act (1986). All studies were approved by the Ethical Review Process Applications Panel of the University of Glasgow or Oxford and conform to the ARRIVE guidelines. Experiments were performed on adult male and female mice aged 7 to 16 weeks at the start of the experiments. All experimental cohorts contained a mix of male and female mice, apart from the cohort of Mrgprd^{CreERT2};Ai32 mice that underwent SNI$_{crush}$ surgery, which was exclusively female. Details of transgenic lines are provided in **Table 1**. Tamoxifen was administered by i.p. injection of 20 mg/mL tamoxifen (Sigma-Aldrich) dissolved in wheat germ oil (doses described in **Table 1**). There were 2 instances where animals were excluded from data analysis: One (cyan fluorescent protein) Thy1-CFP died of unknown causes not related to the procedure and before the experimental endpoint, and one MrgD^{CreERT2};Ai32 exhibited no fluorophore expression and was therefore deemed to have been incorrectly genotyped. Group sizes were based on the extent of neuronal loss 28d following sciatic nerve transection identified by Shi et al.[50] Given $\alpha = 0.05$, power = 0.8, and an effect size of 4.81, power analysis projects that a group size of 3 mice would be needed.

2.2. Spared nerve transection and crush surgeries

Spared nerve injury (transection of the common peroneal and tibial branches of the sciatic nerve; SNI$_{trans}$) and common peroneal and tibial crush injury (SNI$_{crush}$), in which nerve axons were severed but the epineurium remained intact, were performed as previously described.[12] Anesthesia was induced with 3% to 5% isoflurane and then maintained at 1.5% to 2% as required. Analgesia, consisting of carprofen (10 mg/kg) and buprenorphine (0.05 mg/kg) (Glasgow) or carprofen (5 mg/kg) and local bupivacaine (2 mg/kg) (Oxford) was provided perioperatively. The left hindpaw was secured with tape in hip abduction, and the operative field (lateral surface of the thigh) was shaved. Ophthalmic ointment was applied to the eyes, and the shaved area was swabbed with chlorhexidine solution. A longitudinal incision was made in the skin at the lateral mid-thigh. Using blunt dissection, an opening was made through the biceps femoris, exposing the sciatic nerve and the 3 peripheral branches (sural, tibial, and common peroneal nerves). For SNI$_{trans}$, the common peroneal and tibial nerves were ligated using a 6-0 Vicryl suture (Ethicon, Raritan, NJ), and a 1- to 2-mm piece distal to the suture was removed using spring scissors. For SNI$_{crush}$, the exposed tibial and common peroneal nerves were clamped using a pair of fine hemostats (Fine Science Tools, Heidelberg, Germany) closed to their second clip, leaving the nerve branches intact but translucent. The muscle was closed with one 6-0 Vicryl suture (Ethicon), and the skin incision was closed with one 10 mm wound clip (Alzet, Cupertino, CA). Animals were monitored daily for self-mutilation, and no animals required sacrifice due to tissue damage.

Table 1

Transgenic lines used in the study.

Used name	Full name	Putative population	Ref	Source	Tamoxifen regime
Atf3^{CreERT2}	Atf3$^{tm1.1(cre/ERT2)Msra}$	Axotomised afferents	13	Gift: Dr Franziska Denk	50 mg/kg on days 0, 3, and 7 after surgery
Avil^{FlpO}	Avil$^{tm1(flpo)Ddg}$	Sensory neurons	1	Gift: Prof David Ginty	N.A.
MrgD^{CreERT2}	Mrgprd$^{tm1.1(cre/ERT2)Wql}$	Major class of nonpeptidergic neurons	39	The Jackson Laboratory (RRID: IMSR_JAX:031286)	General: 1x 50 mg/kg in adulthood, (>1 week before experiment) 3D volumetric analysis: 5x i.p. (0.5 mg/animal/day), beginning between P10 and P17
MrgD$^{ChR2-YFP}$	Mrgprd$^{tm4.1(COP4)Mjz}$	Major class of nonpeptidergic neurons	59	Mutant Mouse Resource & Research Centers (RRID:MMRRC_036112-UNC)	N.A.
Calca^{CreERT2}	Calca$^{tm1.1(cre/ERT2)Ptch}$	Peptidergic neurons	51	Gift: Prof Pao-Tien Chuang	1x 75 mg/kg in adulthood (>1 week before experiment)
Trpm8^{FlpO}		Cold afferents	4	Gift: Dr Mark Hoon	N.A.
Thy1-CFP	B6.Cg-Tg(Thy1-CFP) 23Jrs/J	Sample of myelinated afferents	16	The Jackson Laboratory (RRID: IMSR_JAX:003710)	N.A.
Th^{CreERT2}	Th$^{tm1.1(cre/ERT2)Ddg}$/J	C low threshold mechanoreceptors	1	Gift: Prof David Ginty; The Jackson Laboratory (RRID:IMSR_JAX:025614)	1x 50 mg/kg in adulthood (>2 weeks before experiment)
RC::FLTG	B6.Cg-Gt(ROSA) 26Sor$^{tm1.3(CAG-tdTomato,-EGFP)Pjen}$/J	Flp-mediated tdTomato; Cre+Flp-mediated GFP expression	40	The Jackson Laboratory (RRID: IMSR_JAX:026932)	N.A.
Ai14	B6.Cg-Gt(ROSA) 26Sor$^{tm14(CAG-tdTomato)Hze}$/J	Cre-mediated tdTomato expression	33	The Jackson Laboratory (RRID: IMSR_JAX:007914)	N.A.
Ai32	B6.Cg-Gt(ROSA) 26Sor$^{tm32(CAG-COP4*H134R/EYFP)Hze}$	Cre-mediated ChR2-eYFP expression	32	The Jackson Laboratory (RRID: IMSR_JAX:024109)	N.A.

CFP, cyan fluorescent protein; GFP, Green fluorescent protein; YFP, yellow fluorescent protein.

2.3. FastBlue tracer injections

Mice were briefly anesthetized during the procedure, induced with 3% to 5% isoflurane, and then maintained at 1.5% to 2% as required. Hindlimbs were taped with the plantar surface of the paw facing up, and a custom, 26G removable needle with a 30° bevel, attached to a 25-μL Hamilton syringe, was inserted between the 2 distal-most footpads, towards the medial aspect of the hindpaw. The needle was then rotated 90°, so the bevel faced medially. Furthermore, 4-μL FastBlue (FB; 2% in sterile phosphate-buffered saline (PBS); CAS# 73819-41-7; Polysciences, Inc, Warrington, PA) per paw was then slowly injected, and the needle was left in place for 10 seconds, before rotating and carefully retracting to avoid backflow of FB along the needle track. This prevented the FB bolus from contacting the sural innervation territory of the lateral hindpaw, restricting it largely to the tibial innervation territory of the glabrous hindpaw skin.

2.4. Immunohistochemistry and image acquisition

Mice were anesthetized with an overdose of pentobarbital (20 mg) and transcardially perfused with a fixative containing 4% formaldehyde. L3 to L5 DRGs were removed and postfixed for another 2 hours, cryoprotected in 30% sucrose overnight, and then embedded in optimal cutting temperature media (OCT; Tissue Tek, Alphen aan den Rijn, the Netherlands). Dorsal root ganglia were sectioned on a Leica CM1950 cryostat at 30 μm, with every section collected serially on 5 Superfrost Plus slides (VWR, Lutterworth, United Kingdom) and each slide containing 1 in every 5 sections (4-7 sections per slide). One slide per DRG was selected at random and was washed with PBS, before being incubated with appropriate primary antibodies (**Table 2**) diluted in 5% normal donkey serum and 0.3% Triton X-100 in PBS for 3 days at 4°C. After PBS washes, slides were incubated with appropriate secondary antibodies (**Table 2**) in the same PBS/(normal donkey serum) NDS/Triton-X100 solution as for primaries, overnight at room temperature. Slides were washed and coverslipped with VectaShield Vibrance Hardset mounting media (Vector Labs, Newark, CA), with 4',6-diamidino-2-phenylindole included in mounting media where FB-labelled cells were not being examined. Sections were imaged using a Zeiss LSM900 Airyscan confocal microscope equipped with 405-, 488-, 561-,

Table 2

Primary and secondary antibodies used in the study.

Antibody	Source	Identifiers	Working dilution
Anti-GFP (Chicken polyclonal)	Abcam, plc, Cambridge, United Kingdom	Cat#: ab13970 RRID: AB_300798	1:1000
Anti-NeuN (Guinea pig polyclonal)	Synaptic Systems, Göttingen, Germany	Cat#: 266004 RRID: AB_2619988	1:500
Anti-mCherry (Rat monoclonal)	Invitrogen, Waltham, MA; Thermo Fisher Scientific, United Kingdom	Cat#: M11217 RRID: AB_2536611	1:500
Anti-Atf3 (Rabbit polyclonal)	Novus Biologicals, Minneapolis, MN	Cat#: NBP1-85816 RRID: AB_11014863	1:500
Anti-NF200 (Rabbit polyclonal)	Sigma-Aldrich, Saint Louis, MO	Cat#: N4142 RRID: AB_477272	1:1000
Anti-TrkA (Goat polyclonal)	R&D Systems, Minneapolis, MN	Cat#: AF1056 RRID: AB_2283049	1:500
Anti-TDP43 (Rabbit polyclonal)	Abcam, plc, Cambridge, United Kingdom	Cat#: ab133547 RRID: AB_2920621	1:100
Anti-RFP (Mouse monoclonal)	Thermo Fisher Scientific, United Kingdom	Cat#: MA5-15257 RRID: AB_10999796	1:200
Anti-RFP (Chicken polyclonal)	Sigma-Aldrich, United Kingdom	Cat#: AB3528 RRID: AB_11212735	1:200
Alexa Fluor 488 Donkey Anti-Chicken IgY (Donkey polyclonal)	Jackson ImmunoResearch, Ely, United Kingdom	Cat#: 703-545-155 RRID: AB_2340375	1:500
Alexa Fluor 647 Donkey Anti-Guinea pig IgG (Donkey polyclonal)	Jackson ImmunoResearch, Ely, United Kingdom	Cat#: 706-605-148 RRID: AB_2340476	1:250
Rhodamine Red-X Donkey Anti-Rat IgG (Donkey polyclonal)	Jackson ImmunoResearch, Ely, United Kingdom	Cat#: 712-295-153 RRID: AB_2340676	1:100
Alexa Fluor 647 Donkey Anti-Rabbit IgG (Donkey polyclonal)	Jackson ImmunoResearch, Ely, United Kingdom	Cat#: 711-605-152 RRID: AB_2492288	1:250
Rhodamine Red-X Donkey Anti-Rabbit IgG (Donkey polyclonal)	Jackson ImmunoResearch, Ely, United Kingdom	Cat#: 711-295-152 RRID: AB_2340613	1:100
Alexa Fluor 546 Goat Anti-Chicken IgG (Goat polyclonal)	Thermo Fisher Scientific, United Kingdom	Cat#: A11040 RRID: AB_2534097	1:400
Alexa Fluor 488 Goat Anti-Rabbit IgG (Goat polyclonal)	Thermo Fisher Scientific, United Kingdom	Cat#: A11008 RRID: AB_143165	1:400
Alexa Fluor 546 Donkey Anti-Mouse IgG (Donkey polyclonal)	Thermo Fisher Scientific, United Kingdom	Cat#: A10036 RRID: AB_2534012	1:400

GFP, green fluorescent protein; RFP, red fluorescent protein

and 640-nm diode lasers. Full thickness, tiled, confocal image stacks with a 2- to 3-μm interval in the Z-axis were obtained through a 20× dry lens (0.8 NA) with the confocal aperture set to 1 Airy unit or less. All image capture was performed using Zen Blue Edition software (Carl Zeiss Microscopy GmbH, Jena, Germany), and analyses were performed using Zen Blue or FIJI.[45]

2.5. Image analysis

During all image quantification, the experimenter was blind to the experimental groups. For quantification of the total number of cells within the DRG, a modified optical dissector stereological method was used[11,18,47] (Fig. S1, http://links.lww.com/PAIN/C84). To account for tissue shrinkage during processing, the mean thickness (t) of each section on one slide (ie, 1 in 5 sections) was calculated by taking the mean of the thickest and thinnest cell-containing regions (ie, not fiber tract-containing regions) of the section (NB: no optical correction to thickness was applied; given the use of a dry lens, this value will not reflect actual section thickness, though this was kept consistent throughout the study). The cell-containing, cross-sectional area (a) was then calculated, using the middle optical section from the series and drawing around the cell-containing regions. Section volume (V_{sec}) was then calculated:

$$Vsec = t \times a$$

Using the Cavalieri principle, the cell-containing volume of the DRG was calculated[11]:

$$VDRG = \bar{a} \times \bar{t} \times l$$

where $\bar{a}$ = mean cell-containing cross-sectional area, $\bar{t}$ = mean section thickness, and l = "length" of the DRG (determined from the total number of sections collected). The number of neurons per section (N_{sec}) was quantified in all immunostained sections. This included only neurons with a visible nucleus (in the NeuN channel), excluded cells with a nucleus visible within the top frame of the Z-stack, and included any neurons with a nucleus visible in any other field within Z-stack, including the bottom frame of Z-stack. The cell density or the number of cells per unit vol (N_v) was then calculated:

$$N_v = \frac{Nsec}{Vsec}$$

Finally, the total number of cells per DRG (N_{DRG}) was calculated:

$$N_{DRG} = \overline{N_v} \times V_{DRG}$$

For quantification of the proportion of FB-labelled cells co-labelled with afferent subpopulation markers, initially, the total number of FB-filled neuronal cell profiles with a visible nucleus anywhere within the section was counted, with the observer blind to other channels. The other channel was then revealed, and instances of co-labelling were quantified. No stereological correction was applied, given that the similar size of neuronal nuclei would prevent over-counts of large neurons and that no comparisons of the total number of labelled cells were made. For soma area analyses, the area of neuronal soma expressing the appropriate marker was measured in the optical section within the Z-stack in which that neuron was at its largest, by drawing around the perimeter of the neuron in Fiji/ImageJ v2.14.0/1.54f.

2.6. Tissue clearing and 3D volumetric analyses

Dorsal root ganglia were extracted from animals 4 weeks post-SNI_trans for whole DRG analyses. In this study, tissue was extracted from a combination of MrgD^CreERT2;Ai14, Th^CreERT2;Ai14, and Calca^CreERT2;Ai14 lines (mixed sex).[3] One month after SNI_trans, animals were transcardially perfused with sterile saline followed by a fixative containing 4% formaldehyde. Ipsilateral and contralateral L4 DRG were removed and postfixed for 24 hours on a shaker at room temperature before being washed in PBS and stored at −80°C in CI-VM1 (35% dimethyl sulfoxide, 35% ethylene glycol in PBS) until clearing. Tissue clearing was then performed as previously described.[67] In brief, the tissue was exposed to a gradient of 1-propanol containing 0.3% triethylamine (30, 50, 75, 90, 95, 100, 100%) and washed in this solution at 37°C for 24 hours. The tissue was then rehydrated in PBS and labelled with primary antibodies for 1 week at 37°C (mouse anti-TDP43 and 2x anti-RFP, **Table 2**). The tissue was washed for 24 hours and incubated with appropriate secondary antibodies (**Table 2**) for another week at 37°C. The tissue was subsequently washed for 24 hours, dehydrated again in increasing concentrations of 1-propanol containing 0.3% triethylamine, and mounted in benzyl alcohol with benzyl benzoate (1:2 ratio) containing 0.3% triethyl-amine on glass slides with silicone spacers. Imaging was performed on an Olympus spinning disk confocal microscope at 20x, with 2-μm z-steps. The tissue was stored at 4°C for ~16 months before imaging, so only the tissue that remained transparent at this time was used for downstream analyses. Volumetric analyses were performed using Imaris using the "spots" feature with region growth (to allow for different-sized spots), background subtraction, and point spread function elongation (standard 2 × XY). Initial spot diameters were set based on MrgD^CreERT2;Ai14 nuclear size (as labelled by red fluorescent protein (RFP)). Spot classification was then performed blind by adjusting the quality threshold to balance detection in superficial and deep tissue. This step was necessary due to differences in tissue quality after long-term storage. Any labelled spots in the adjacent nerve were then deleted (eg, labelled Schwann cells or debris). Count and volumetric data were then exported for analysis in R. Data were filtered for very small (<5 μm³) and very large (>2000 μm³) spots to further remove any debris, labelled satellite glia or doublets within the ganglia. In both cases, these filters were approximate and did not exclude the possibility that some spots correspond to either class in the final dataset. The upper limit of the "small" DRG nuclei size category was defined as the upper bound of 32 easily identifiable MrgD+ nuclei (258 μm³). The boundary between "medium" and "large" bins (400 μm³) was less clearly defined in the samples and was therefore set as the approximate midpoint of the volume distribution. A combined size category for all nuclei greater than 258 μm³ was also examined, and the results mirrored those of "medium" and "large" bins.

2.7. Gene Ontology

Gene Ontology term analyses were performed on previously published mouse subtype RNA-seq after SNI (GSE216444[3]). In this study, subtype-specific bulk RNA-seq was performed on 5 transgenic mouse lines through reporter labelling and fluorescence activated cell sorting. spliced transcripts alignment to a reference was used to map reads to the GRCm38 (mm10) Mouse Genome,[14] and Samtools was used to sort, index, and merge Binary Alignment Map files in line with published reports.[28] Quality control was performed as per Barry et al.[3] Downstream analyses were performed using DESeq2 on grouped male and female samples.[31] For differentially expressed genes (false discovery rate) (FDR < 0.05, LFC >1) (log-fold change), GO analyses were performed using the Wallenius method using goSeq (R). In this study, significantly regulated terms related to

cell death and apoptosis with more than 10 genes were examined. Filtered count data of expressed and nondifferentially expressed genes were used as a background.

2.8. Dorsal root ganglion culture

Dorsal root ganglia were dissected from MrgD^{CreERT2};Ai32 and Calca^{CreERT2};Ai32 mice >1 week after dosing with tamoxifen and enzymatically digested at 37°C for 80 minutes in dispase type II (4.7 mg/mL) plus collagenase type II (4 mg/mL) (Worthington Biochemical), as described previously.[63] Mechanically dissociated cells were plated onto laminin/poly-D-lysine (R&D Systems, Minneapolis, MN) treated coverslips in complete Neurobasal Plus medium (Neurobasal Plus media supplemented with 2% (vol/vol) B27 Plus, 1% N2, 1% Glutamax, and 1% antibiotic–antimycotic [ThermoFisher Scientific, Waltham, MA]). Mouse nerve growth factor (GF) (50 ng/mL; nerve growth factor (NGF), PeproTech, Cranbury, NJ) and 10 ng/mL glial-derived neurotrophic factor (GDNF, PeproTech) were added to the media under some conditions. Cytosine β-D-arabinofuranoside (4 μM) was added to the media for 24 hours the day after plating to reduce the proliferation of nonneuronal cells. Media was refreshed 3 times per week thereafter. Cultures were fixed for 10 minutes at room temperature with 4% paraformaldehyde and subsequently processed by immunocytochemistry (described earlier).

2.9. Statistical analysis

Data are expressed as mean ± SEM unless otherwise specified, and P values of less than 0.05 were considered significant. Power calculations were performed using G*Power 3.1.9.7.[15] A quantitative Venn diagram was created using BioVenn.[25] All other statistical analyses were performed in Prism 10 (GraphPad Software, Inc, Boston, MA) or R using paired t tests or 1- or 2-way RM ANOVAs (repeated measures analysis of variance), where appropriate. Normality was assessed by the Shapiro–Wilk test. If the main analysis of variance effect was significant, Šídák or Tukey multiple comparisons tests were performed. To compare population distributions of soma cross-sectional area or volume, Kolmogorov–Smirnov tests were performed.

3. Results

3.1. Peripheral nerve injury induces a loss of small neurons from the dorsal root ganglion

To assess the gross loss of neurons from DRG following nerve injury, we generated the Avil^{FlpO};Atf3^{CreERT2};RC::FLTG mouse line in which naïve and axotomized sensory neurons were differentially labelled. In this mouse line, all neurons express tdTomato (Flp-dependent) in the naïve state and switch to expressing green fluorescent protein (GFP) upon axonal damage and concurrent tamoxifen treatment (Flp- and Cre-dependent) (**Figs. 1A and B**). Following pilot experiments to optimize tamoxifen dosing regimen, this approach was both highly efficient and specific (with the caveat that it was necessary to wait for several days after nerve injury for Cre-induced GFP expression): 14 days after SNI$_{trans}$ surgery, GFP was expressed by 99.1 ± 0.6% of Atf3-expressing ipsilateral L4 DRG neurons, while we observed GFP in only 4.6 ± 0.7% of contralateral DRG neurons (Figs. S2A–D, http://links.lww.com/PAIN/C84). We then used a stereological approach to quantify the total number of neurons in L4 DRG ipsilateral to injury 1, 2, 4, and 8 weeks after SNI$_{trans}$, as well as contralateral to injury. One week after SNI$_{trans}$, we

observed 7809 ± 153 neurons per DRG; this was not significantly different to the number of neurons in the contralateral DRG (7917 ± 349), whereas cell number approximately halved by 8 weeks postinjury to 3963 ± 410 neurons per DRG (**Fig. 1C**). Separating analysis into intact vs axotomized afferents revealed that only axotomized afferents were lost, with no difference observed in numbers of intact afferents (**Fig. 1D**). Between 1 and 8 weeks after injury, we observed a 61.0 ± 7.0% decrease in the number of GFP+ neurons. This loss of injured afferents resulted in a loss of neuron-containing (ie, excluding white matter regions) DRG volume (**Fig. 1E**), but not neuron density (**Fig. 1F**). Cell loss predominantly occurred between 1 and 2 weeks postinjury and stabilized after this timepoint. Population distributions of the cross-sectional area of nucleated, tdTomato-expressing cell profiles were not significantly different at 1 vs 8 weeks post-SNI$_{trans}$, in contrast to GFP-expressing/injured afferents, in which a loss of a population of small afferents at 8 weeks postinjury was observed (**Fig. 1G**).

SNI$_{trans}$ resulted in a mixed population of axotomized and intact afferents within the L4 DRG. Therefore, we developed an approach to restrict our analysis to axotomized afferents, without relying on transgenic labelling, and used this as a complementary approach to confirm our findings. We injected the neuronal tracer FB into the glabrous, tibial innervation territory of both hindpaws 1 week before common peroneal and tibial transection (SNI$_{trans}$) or crush (SNI$_{crush}$) surgeries (**Figs. 2A and B**). FastBlue-uptake was complete across neurons of all sizes by 1 week (Fig. S3, http://links.lww.com/PAIN/C84), so this approach allowed us to profile a sample of the axotomized afferents. Both SNI$_{trans}$ (**Fig. 2C**) and SNI$_{crush}$ (**Fig. 2D**) injuries resulted in a rightward shift in population distributions of the cross-sectional area of nucleated, FB-labelled DRG neurons when compared with contralateral DRG, consistent with a loss of small afferents post–nerve injury.

As a third complementary approach, we applied semiautomated volumetric analyses of nuclei size following tissue clearing. In this study, whole DRGs were cleared 4 weeks after SNI$_{trans}$ for nuclei counting in "complete" tissue (**Figs. 2E–H**). Nuclei were labelled by TDP-43, in line with the study by West et al.,[67] and were quantified using Imaris software (**Fig. 2F**, Video 1). We observed a slight but significant rightward shift in nuclear spot volume population distribution 4 weeks after SNI$_{trans}$ (**Fig. 2G**). In addition, there was a significant reduction in the number of small but not medium or large nuclear spots, in support of a loss of small-diameter neuron populations (**Fig. 2H**).

Together, our data derived from several different experimental approaches show that a population of small-diameter afferents are lost following peripheral nerve injury.

3.2. Spared nerve crush or transection results in death of Mrgprd-expressing neurons

To date, determining cell loss among specific populations of afferent neurons has proved challenging due to the downregulation of subpopulation-specific marker genes following axonal transection.[37,44] To overcome this issue, we took advantage of transgenic strategies to label populations in a manner that persisted after injury. Owing to the bias for the loss of small neurons and the known loss of IB4-binding central terminals postinjury,[36] we initially focused on nonpeptidergic nociceptive neurons. We used MrgD$^{ChR2-YFP}$ mice to identify neurons belonging to the largest of the 3 classes of nonpeptidergic nociceptors, NP1.[55,59] To determine whether these neurons are lost following nerve injury, we used a stereological method to quantify L4 DRG MrgD-YFP$^+$ (yellow fluorescent
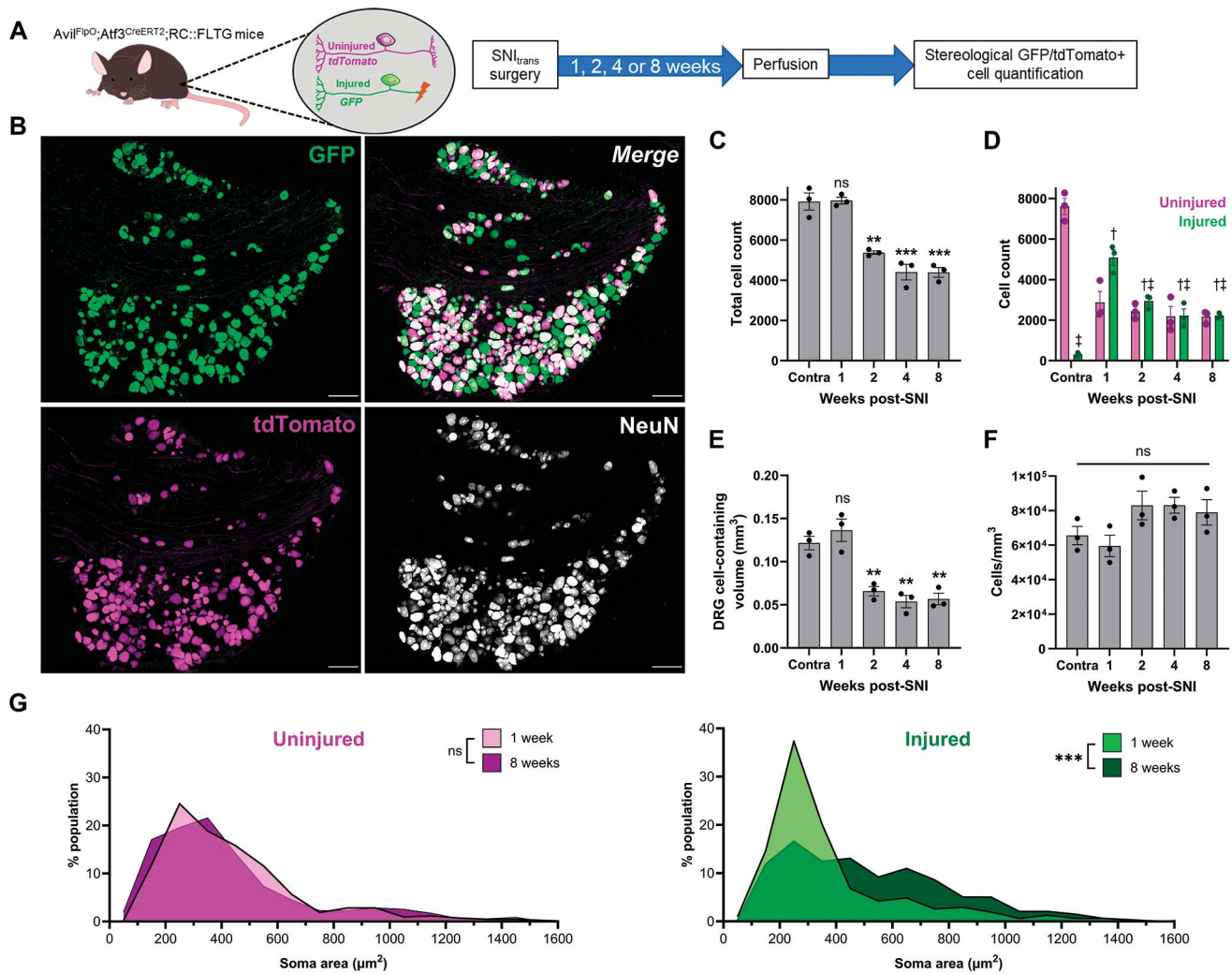
Figure 1. SNI$_{trans}$ induces death of small primary afferent neurons, accompanied by a reduction in volume, not cell density, of the dorsal root ganglion. (A) Approach to differentially labelled intact afferents with tdTomato and damaged afferents with GFP after peripheral nerve injury using the Avil^{FlpO};Atf3^{CreERT2};RC:: FLTG mouse line and schematic of experimental timeline. (B) Representative image of GFP, tdTomato, and NeuN expression in an L4 DRG, 2 weeks after SNI$_{trans}$. Scale bars = 100 μm. (C and D) Stereological quantification of the total number of DRG neurons (C) or number of axotomized and intact neurons (D) in the L4 DRG 1, 2, 4, and 8 weeks after SNI$_{trans}$ or contralateral (contra) to injury. (C) One-way ANOVA with Tukey posttests; $F_{4,10} = 37.98$, $P < 0.001$. (D) Two-way RM ANOVA; Timepoint × Color interaction $F_{4,10} = 39.04$, $P < 0.001$, n = 3 mice; Tukey posttests (between injured groups): †$P < 0.05$ vs contra, ‡$P < 0.05$ vs 1-week. (E) Volume of DRG-containing cells (ie, excluding white matter tracts) following SNI$_{trans}$. One-way ANOVA with Tukey posttests; $F_{4,10} = 21.25$, $P < 0.001$, n = 3. (F) Neuronal density within the DRG following SNI$_{trans}$. One-way ANOVA; $F_{4,10} = 2.77$, $P = 0.09$, n = 3. (G) Population distribution of uninjured and injured afferents by cross-sectional area, 1 and 8 weeks post-SNI$_{trans}$. Kolmogorov–Smirnov tests of cumulative distributions; Uninjured: D = 0.08, $P = 0.18$; Injured: D = 0.32, $P < 0.001$; n = 310 to 427 neurons from 3 mice. *$P < 0.05$, **$P < 0.01$, ***$P < 0.001$ vs contra. ANOVA, analysis of variance; DRG, dorsal root ganglion; GFP, green fluorescent protein.

protein) neurons 28 days after sham surgery or SNI$_{trans}$ (**Figs. 3A and B**). SNI$_{trans}$, but not sham, resulted in a significant decrease (54.0 ± 6.6%) in the total number of MrgD-YFP$^+$ neurons in L4 DRG (**Fig. 3C**).

Yellow fluorescent protein expression in MrgD$^{ChR2-YFP}$ mice is driven by the endogenous *Mrgprd* promotor, which has been reported to be upregulated or downregulated following axonal damage.[44,58] Such changes in promoter activity could affect the proportion of nonpeptidergic nociceptors identified by YFP expression. Therefore, to verify these findings, we used MrgD^{CreERT2};Ai32 mice and tamoxifen administration before injury, to permanently label *Mrgprd*-expressing afferents with ChR2-YFP (**Figs. 3D–F**). We then tested whether the proportion of cutaneous tibial afferents that were YFP$^+$ was altered following nerve injury. Following hindpaw FB injection, ~15% of contralateral, FB-labelled DRG neurons expressed YFP. This was reduced to 6.0 ± 1.2% 28 days after SNI$_{crush}$ injury and to only 1.7 ± 0.9%

28 days after SNI$_{trans}$ (**Fig. 3G**). Uptake by uninjured YFP$^+$ neurons was equivalent 7 and 35 days after FB injection, demonstrating that this reduction was not because 7 days were insufficient for YFP$^+$ neurons to fully uptake FB (Fig. S3C, http:// links.lww.com/PAIN/C84). No significant difference in the percentage of FB-labelled YFP$^+$ DRG neurons between ipsilateral and contralateral DRG was observed at 7 days following SNI$_{trans}$ (Figs. S4A and B, http://links.lww.com/PAIN/C84), demonstrating that loss occurred after this timepoint. Analysis of the cross-sectional soma area of FB-labelled, YFP$^+$ neurons in uninjured DRG revealed an area of 361 ± 138 μm^2 (mean ± SD) (Fig. S4C, http://links.lww.com/PAIN/C84), which is a distribution profile matching those neurons presumed lost. Collectively, these data show that peripheral nerve injury results in a substantial loss of nonpeptidergic, *Mrgprd*-expressing neurons, with SNI$_{trans}$ (ie, an unrepaired axonal transection) resulting in an almost complete loss of this population.
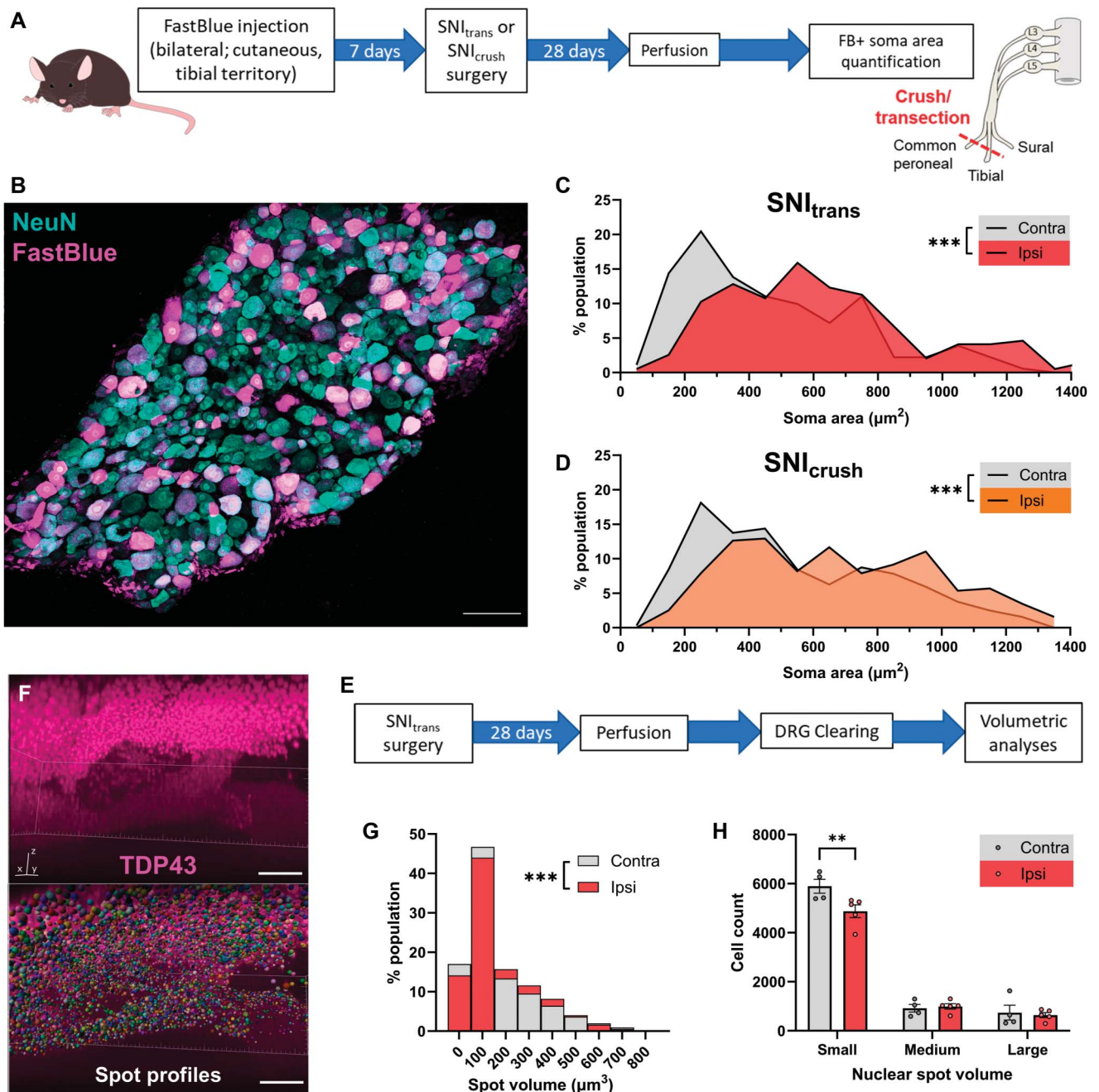
Figure 2. Spared nerve crush and transection lead to a loss of small DRG neurons. (A) Approach to restrict analysis to damaged afferents: a subcutaneous injection of the tracer FB into both hindpaws labelled tibial afferents, before unilateral SNI$_{trans}$ or SNI$_{crush}$ surgery. (B) Representative image of FB labelling and NeuN immunostaining in the L4 DRG. The image is a projection of optical sections at 3-μm intervals through the entirety of a 30-μm-thick tissue section. Scale bar = 100 μm. (C and D) Quantification of the cross-sectional area of FastBlue labelled DRG neurons ipsilateral and contralateral to SNI$_{trans}$ (C) or SNI$_{crush}$ injury (D) reveals a loss of small afferents and subsequent shift in population distribution. Kolmogorov–Smirnov tests of cumulative distributions; SNI$_{trans}$: D = 0.25, $P <$ 0.001; n = 183 or 191 neurons from 3 mice; SNI$_{crush}$: D = 0.22, $P <$ 0.001, n = 319 or 325 neurons from 3 mice. (E) Experimental approach for whole DRG volumetric analyses after SNI$_{trans}$. (F) Representative 3D rendering of TDP-43 profiles and corresponding nuclear spot profiles following Imaris-based spot detection feature. Scale bar = 100 μm. (G) Quantification of DRG nuclear spot volume ipsilateral and contralateral to SNI$_{trans}$. Kolmogorov–Smirnov tests of cumulative distribution: D = 0.06, $P <$ 0.001, n = 30,206 (contra) or 32,544 (ipsi) nuclei from 4 (contra) or 5 (ipsi) mice. (H) Total number of nuclear spots, by size, per DRG. Two-way RM ANOVA; size bin × injury interaction: $F_{2,14}$ = 8.26, P = 0.004; n = 4 to 5 mice; Šídák multiple comparisons tests: **$P <$ 0.01. ANOVA, analysis of variance; DRG, dorsal root ganglion; FB, FastBlue; RM, repeated measures.

3.3. Spared nerve injury induces a loss of Trpm8$^+$ and calcitonin gene-related peptide$^+$ but not myelinated dorsal root ganglion neurons

Loss restricted to nonpeptidergic nociceptors would not fully account for the degree of total neuron loss that we observed. Therefore, we studied a range of other subpopulations, both small and large in diameter, for their vulnerability to injury-induced loss. To investigate potential loss of Trpm8$^+$ (cold-sensitive), calcitonin gene-related peptide$^+$ (CGRP) (peptidergic), and myelinated subpopulations of DRG neurons following nerve injury, we applied our FB-labelling approach in Trpm8^{FlpO}; RC::FLTG (FlpO-dependent tdTom expression), Calca^{CreERT2}; Ai32 (Cre-dependent ChR2-YFP expression) and Thy1-CFP mice, respectively (**Figs. 4A–D**). Trpm8-tdTom was expressed
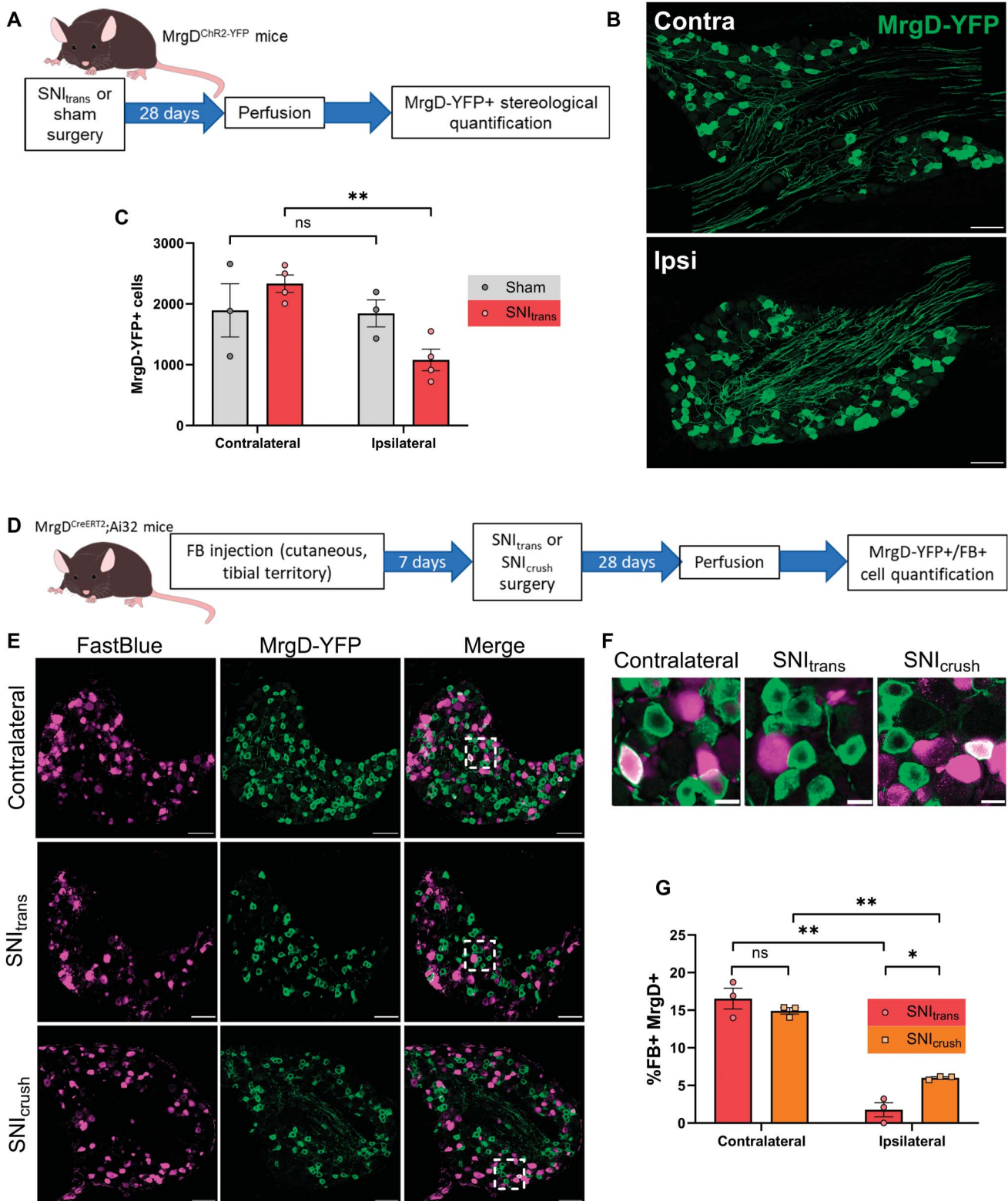
Figure 3. Spared nerve crush or transection results in death of nonpeptidergic neurons. (A) Schematic of experimental approach for (B and C). (B) MrgD^ChR2-YFP L4 DRGs 4 weeks after SNI, contralateral or ipsilateral to injury. Images are projections of optical sections at 3-μm intervals through the entirety of 30-μm-thick tissue sections. Scale bars = 100 μm. (C) Quantification of total number of MrgD-YFP+ cells per L4 DRG 4 weeks after SNI revealed a significant loss in ipsilateral DRG. Two-way RM ANOVA with Šídák multiple comparisons tests; Side x Treatment interaction: $F_{1,5} = 9.23$, $P = 0.029$; n = 3 mice. (D) The experimental approach used to generate data presented in (E–G). (E and F) MrgD-YFP expression and FB labelling in the L4 DRG, 14 days after SNI or crush surgery or contralateral to injury. White boxes represent regions enlarged in (F). Scale bars = 100 μm (E) or 20 μm (F). (G) The proportion of FB-labelled DRG neurons decreased after spared nerve crush injury, and co-labelling is almost completely absent after SNI. Two-way RM ANOVA with Šídák multiple comparisons tests; side × injury interaction: $F_{1,4} = 7.80$, $P = 0.049$; n = 3 mice. Posttests: *$P < 0.05$, **$P < 0.01$. ANOVA, analysis of variance; DRG, dorsal root ganglion; SNI, spared nerve injury; FB, FastBlue; RM, repeated measures.
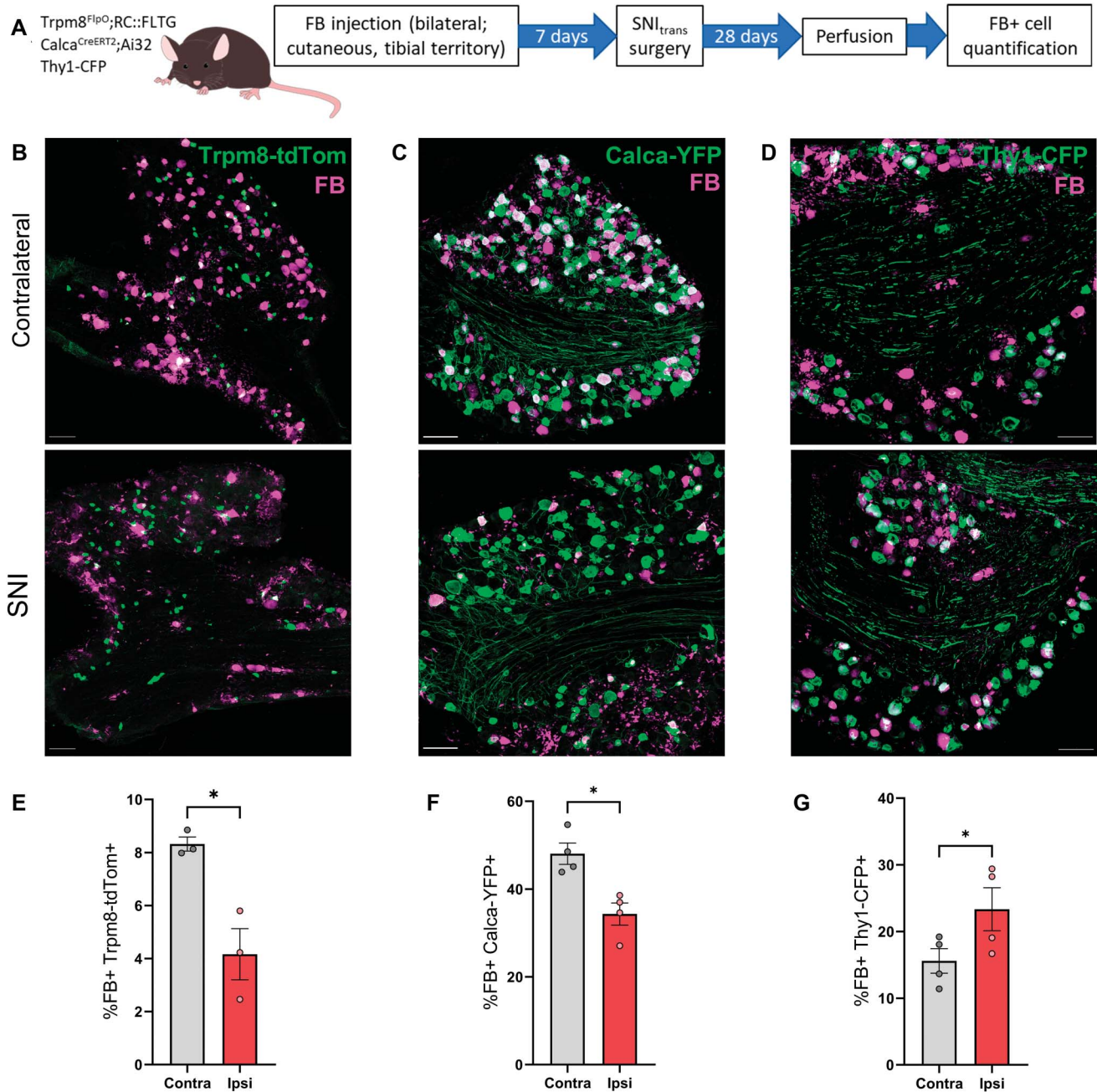
Figure 4. Spared nerve injury induces a loss of Trpm8+ and CGRP+ but not myelinated DRG neurons. (A) Schematic of experimental approach. (B–D) FastBlue labelling and Trpm8-tdTom (B), Calca-YFP (C), or Thy1-CFP expression (D) 28 days after SNI$_{trans}$ in the L4 DRG, contralateral (top) or ipsilateral (bottom) to injury. Images are projections of optical sections at 3-μm intervals through the entirety of 30-μm-thick tissue sections. Scale bars = 100 μm. (E–G) Quantification of the proportion of FB-labelled neurons also expressing Trpm8-tdTom (E), Calca-YFP (F), or Thy1-CFP (G) in L4 DRG contralateral or ipsilateral to SNI$_{trans}$. Paired t tests; Trpm8-tdTom: $t_2 = 5.31$, $P = 0.034$, n = 3 mice; Calca-YFP: $t_3 = 4.12$, $P = 0.026$, n = 4 mice; Thy1-CFP: $t_3 = 4.42$, $P = 0.022$, n = 4 mice. *$P < 0.05$. CFP, cyan fluorescent protein; CGRP, calcitonin gene-related peptide; DRG, dorsal root ganglion; FB, FastBlue.

by a population of small-diameter, putative cold-sensitive neurons (**Fig. 4B**), accounting for 8.3 ± 0.27% of FB-labelled neurons in contralateral DRG. This decreased to 4.2 ± 0.96% ipsilateral to SNI$_{trans}$ injury (**Fig. 4E**), indicating a partial loss of Trpm8$^+$ afferents. When examining peptidergic afferents, we found that 48.1 ± 2.42% of FB-labelled neurons in contralateral DRG were Calca-YFP$^+$, compared with 34.3 ± 2.54% 4 weeks after SNI$_{trans}$ injury (**Figs. 4C and F**), consistent with a partial loss of CGRP$^+$ afferents. We used a Thy1-CFP line that demonstrates consistent expression postinjury[61] and labels a sample of medium/large diameter myelinated afferents. CFP was largely restricted to NF200$^+$ neurons, labelling 56% of this population.

Expression was present in a heterogenous population of nociceptive (TrkA+) and nonnociceptive (TrkA-) myelinated neurons (Fig. S5, http://links.lww.com/PAIN/C84). Contralateral to injury, 15.6 ± 1.8% of FB-labelled neurons expressed Thy1-CFP (**Figs. 4D and G**). In contrast to unmyelinated subpopulations, this proportion was higher in ipsilateral DRG following SNI$_{trans}$ (23.3 ± 3.2%), consistent with no (or minimal) loss of Thy1-CFP-expressing afferents, accompanied by a loss of Thy1-CFP-negative neurons. We did not observe significant alterations in the population distributions of the cross-sectional area of surviving, damaged Trpm8-tdTom$^+$, Calca-YFP$^+$, or Thy1-CFP$^+$ DRG neurons when compared with DRG contralateral to

injury (Fig. S6A–C, http://links.lww.com/PAIN/C84), indicating that any loss of neurons within specific neuronal subpopulations was not biased towards soma size. Collectively, these data show that unrepaired axonal damage to peripheral sensory neurons induces a partial loss of Trpm8$^+$ and CGRP$^+$ subpopulations, but no major loss of myelinated afferents.

Based on our findings of preferential loss of nonpeptidergic nociceptors, we re-analyzed a previous population-specific transcriptomic dataset of mouse DRG neurons following nerve injury for potential upregulation of cell death pathways (Fig. S7, http://links.lww.com/PAIN/C84).[3] We found that early after injury (3 days post-SNI$_{trans}$), nonpeptidergic (MrgD^{CreERT2}-expressing) neurons showed enhanced enrichment of GO terms associated with apoptosis, in contrast to a broad population of nociceptors (labelled with Scn10a^{CreERT2}), peptidergic nociceptors (Calca-^{CreERT2}), C-LTMRs (Th^{CreERT2}), and Aβ-RA (rapidly adapting) and Aδ-LTMRs (Aδ/Aβ-LTMR, Ntrk2^{CreERT2};Advillin^{FlpO}), in which there was less or no enrichment of cell death pathways. By 4 weeks, only C-LTMR and Aδ/Aβ-LTMR subtypes show any overrepresentation of cell death pathways (in the populations studied). Both injury-specific and apoptotic signatures in non-peptidergic neurons were no longer significantly enriched, consistent with a loss of axotomized nonpeptidergic afferents by this late timepoint postinjury. These data suggest that apoptotic pathways are upregulated acutely after injury in a cell-type-specific manner.

3.4. Mrgprd dorsal root ganglion neurons are sensitive to loss in vitro

Earlier studies postulated that a lack of neurotrophic support underlies neuronal loss, which is supported by the observation that exogenous GDNF treatment at the time of injury, or shortly after, rescues the loss of IB4-binding central terminals posttransection.[5] We sought to use the DRG neurons from MrgD^{CreERT2};Ai32 mice to test this postulate and establish an in vitro platform capable of probing the molecular basis of loss, with axonal transection during isolation providing a correlate for in vivo nerve injury (**Figs. 5A–E**). Twenty-four hours after plating, YFP was expressed by 16.3 ± 1.3% of DRG neurons, which was reduced to 11.8 ± 1.7% after 28 days of culture in the presence of exogenous GFs, NGF and GDNF (**Fig. 5F**). However, in the absence of GFs, YFP$^+$ neurons only accounted for 1.7 ± 0.6% of neurons after 28 days, accompanied by an apparent reduction in the overall number of neurons within the culture, despite all conditions being seeded at the same initial density (**Figs. 5C and F**). YFP$^+$ cell loss was partially rescued by the presence of GDNF, but not NGF alone, in the culture media (**Figs. 5D–F**). These results contrasted with experiments using neurons derived from Calca^{CreERT2};Ai32 mice, in which we observed no change in the proportion of neurons that were Calca-YFP$^+$ after 28 days in culture, regardless of exogenous GF addition (**Figs. 5G–L**). Collectively, these data support the use of DRG cultures to probe the mechanisms underlying selective loss of sensory neurons following nerve injury and suggest a role for trophic support, particularly by GDNF signaling, in preventing the loss of nonpeptidergic nociceptors.

4. Discussion

We present data herein to support the hypothesis that traumatic nerve injury in rodents leads to a profound loss of small-diameter DRG neurons. Taking advantage of newly developed transgenic recombinase driver lines, we have shown that loss is biased across molecularly defined subpopulations. Nonpeptidergic nociceptive neurons are particularly susceptible to loss, with almost all Mrgprd$^+$ axotomized afferents lost following an unrepaired transection injury (SNI$_{trans}$) and roughly half lost following a model which contrastingly allows for nerve regenerations (SNI$_{crush}$). Finally, we have observed that the vulnerability of Mrgprd$^+$ neurons extends to the in vitro setting and provide data to support the hypothesis that loss is driven by a lack of neurotrophic support following injury.

4.1. Neuronal loss

The question of whether DRG neurons die following traumatic injury has been addressed by several groups over the last few decades. Despite contrasting findings on the extent, timing, and form that loss takes, most studies have observed frank loss of DRG neurons.[6,38,46,53] However, more recent studies using recombinase driver lines and novel machine-learning approaches have cast doubt on this consensus.[44,49] Our data strongly support the loss hypothesis and suggest that approximately 60% of axotomized afferents die within 2 weeks of SNI. The discrepancy between our findings and other recent studies may be partly explained by the sampling method used to estimate neuronal numbers. For example, Schulte et al.[49] developed a novel machine-learning approach and found no reduction in neuron density across serial sections of rat DRG following SNI, and they inferred from this that frank loss did not occur. Our results are congruous, in that we also observed no reduction in neuron density. However, we found a substantial loss in the total neuron-containing volume of injured DRG, which underlies our contrasting conclusion of frank loss. Of note, morphological volumetric analysis and MRI have also previously demonstrated volume loss in both rodent and human DRG following nerve injury.[35,65,66] These findings occur despite a major increase of nonneuronal cells in the injured DRG[30] and support the notion that the total DRG neuron number is decreased.

4.2. Selectivity of neuron loss

While definitively characterizing loss of molecularly defined subpopulations was challenging before the advent of recombinase driver lines, a consensus emerged that small-diameter neurons are more vulnerable to nerve injury–induced loss.[50,53] Our data support this consensus and extend it to reveal that while there is a generalized partial loss of C-fiber populations including CGRP- and Trpm8-expressing neurons, Mrgprd-expressing neurons are particularly sensitive to loss. This selective vulnerability has been hinted at previously by the stark reduction in the number of DRG neurons and their central terminals that bind IB4 and express canonical markers such as the P2X$_3$ receptor following nerve injury.[5,8,29,36] Type 1a glomeruli are also reduced in lamina II, suggesting a structural loss of central terminals and not simply a loss of IB4-binding.[2] However, it was not clear whether these data represented phenotypic changes in non-peptidergic nociceptors or frank loss of neurons. We describe neuron loss that is delayed (occurring >7 days postinjury) with respect to histochemical and structural changes (occurring 1-5 days postinjury[2,29]), suggesting that these changes precede and are not in themselves indicative of neuron loss.

The vulnerability of Mrgprd-expressing neurons is congruous with recent subpopulation bulk RNA-seq data, which found that
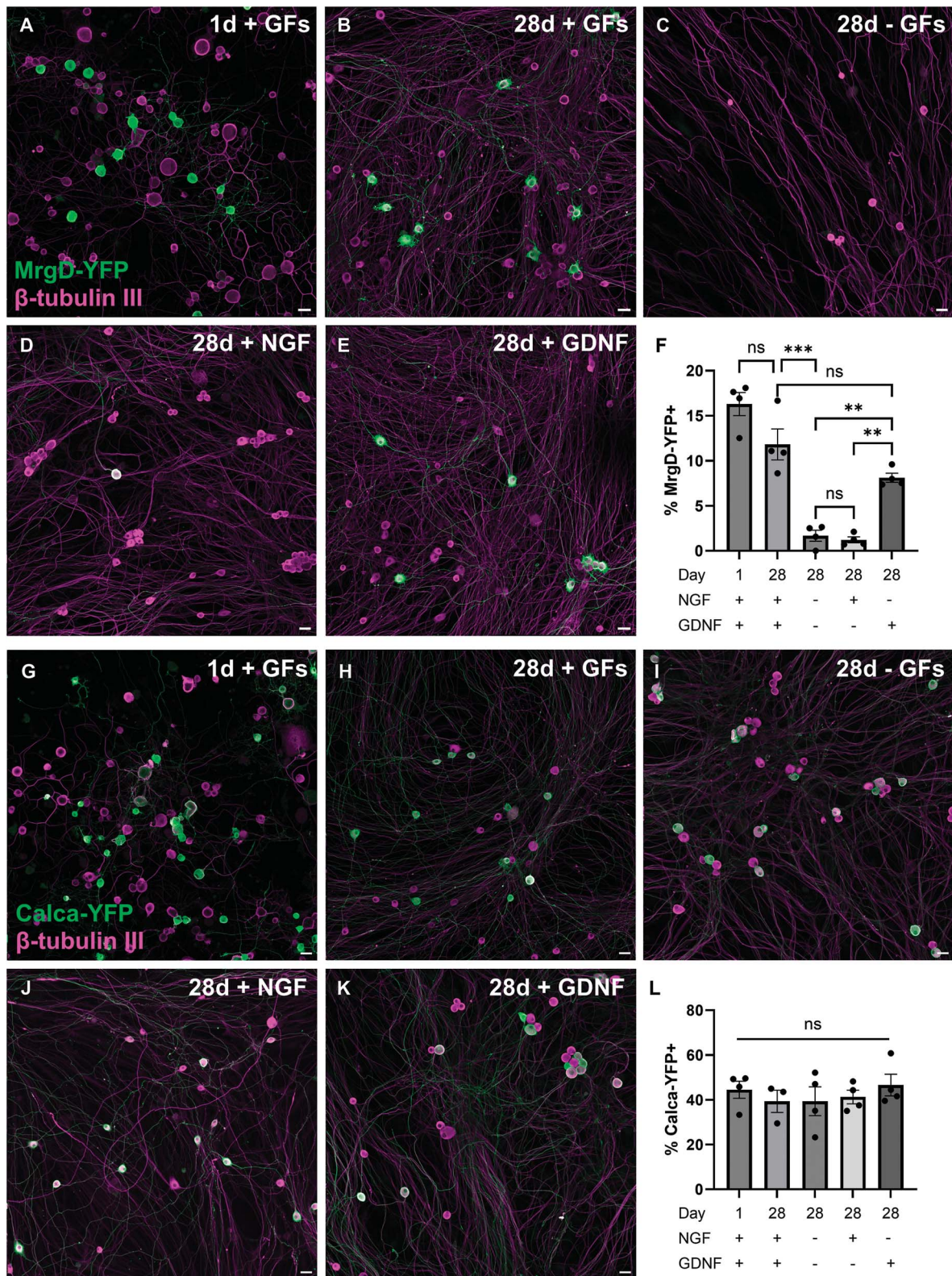
Figure 5. Neurotrophic support ameliorates MrgD+ cell loss in vitro. (A–E) Representative fields of view of MrgD-YFP and β-tubulin III expression in neuronal cultures of isolated MrgD^{CreERT2};Ai32 DRGs, 24 hours (A) or 4 weeks (B–E) after plating, with the addition of the growth factors (GFs) NGF, GDNF, both, or neither. Scale bars = 20 μm. (F) Quantification of the percentage of neurons that express MrgD-YFP under the conditions shown in (A–E). One-way ANOVA with Tukey posttests; $F_{4,15} = 39.7$, $P < 0.001$; n = 4 mice. Posttests: $^*P < 0.05$, $^{**}P < 0.01$, $^{***}P < 0.001$. (G–K) Representative fields of view of Calca-YFP and β-tubulin III expression in neuronal cultures of isolated Calca^{CreERT2};Ai32 DRGs, with the addition of NGF, GDNF, both, or neither. Scale bars = 20 μm. (L) Quantification of the percentage of neurons that express Calca-YFP. One-way ANOVA; $F_{4,14} = 0.46$, $P = 0.76$; n = 3 to 4 mice. ANOVA, analysis of variance; DRG, dorsal root ganglion; GDNF, glial-derived neurotrophic factor; NGF, nerve growth factor; YFP, Yellow fluorescent protein.

SNI-related gene expression signatures were less evident in Mrgprd-expressing and C-LTMR neurons at later timepoints, compared with other populations in injured DRG.[3] This could be explained by a loss of axotomized neurons of these classes and therefore sampling of only uninjured neurons at this time-point.[24,43,64] In terms of the transcriptional response to injury, nonpeptidergic nociceptors show enrichment of individual proapoptotic factors early after injury,[23,68] and we extend these results in this study, by describing a subpopulation-specific enrichment of GO terms associated with apoptosis that is evident as early as 3 days after injury. Such data and single-cell transcriptomic profiling of all DRG neurons following injury[37,44] may offer the opportunity to elucidate the cell death pathways engaged and upstream effectors that enrich this process to nonpeptidergic nociceptive neurons.

4.3. Implications for pain pathogenesis

Neuronal loss has been proposed as a key contributor to poor functional recovery following nerve injury,[54] and biased survival of different afferent types might be expected to contribute to modality-specific sensory deficits. Beyond loss of function, does DRG neuron loss contribute to chronic pain, in either an adaptive or maladaptive manner? Intrathecal delivery of GDNF is neuro-protective and reverses the reduction in the number of IB4-binding DRG neurons and central terminals seen following transection.[5] Treatment is concurrently analgesic and abrogates pain-related behaviors.[7,60] However, the pleiotropic nature of GDNF makes it impossible to directly attribute the analgesic effects to the reversal of neuron loss. Indeed, it is possible that GDNF exerts its effect by actions on intact nonpeptidergic nociceptive afferents,[52] activation of which is known to drive aversive behaviors in the neuropathic state.[62] These data leave the contribution of nonpeptidergic nociceptor loss to behavior in the GDNF treatment paradigm ambiguous. Other pharmacological approaches have been found effective at reversing a neuronal loss in rodent models, but the impact on pain behavior was not studied.[21,22]

Rodents develop marked mechanical and thermal hypersen-sitivity rapidly following nerve injury and before timepoints at which neuron loss is observed.[10] This lack of a temporal correlation may suggest a limited contribution to evoked hyper-sensitivities. The temporal profile of ongoing tonic pain (eg, pain aversiveness as measured by condition place preference assays[26]) is less defined and so is its correlation to the timing of neuron loss.

There are many anatomical sites within the somatosensory nervous system where differential loss of sensory neuron populations could impact neurobiology. For example, loss of cutaneous afferents may afford more opportunity for plasticity in reinnervation patterns, such as collateral sprouting of uninjured or surviving afferents, and the types of nerve endings made by different molecular subpopulations.[17,27] It also seems likely that the death of many neurons within a DRG could contribute to the expansion and activation of immune cell types, which are known to play a major role in neuropathic pain.[30,69] Finally, under normal conditions, peripheral sensory input is integrated into the dorsal horn of the spinal cord by complex interneuron circuitry. Many spinal circuits are engaged by convergent input from different afferent types.[9,41,70] Therefore, selective loss of input from discrete afferent types could undoubtedly impact the normal processing of remaining afferent signals.[34] Experimentally abrogating neuronal loss may be a fruitful approach to assess the contribution to nervous system plasticity (adaptive or maladaptive) following injury. In this regard, our in vitro readout would be a useful experimental

platform to help delineate the precise cell death pathways and signaling cascades engaged (which could then be experimentally manipulated). Such studies should consider that plasticity may evolve over time. The loss of IB4$^+$ central terminals is transient following crush and has even been observed to reverse at longer timepoints following SNI$_{trans}$.[36] These observations, in conjunction with ours of loss of neurons, raise the intriguing question of the source of such central reinnervation.

4.4. Study limitations

Our efforts focused on traumatic nerve injury paradigms owing to previous contrasting results using these robust and reproducible experimental models. We did not extend our studies to systemic neuropathy models, such as chemotherapy or diabetic neurop-athy. A recent postmortem analysis reported a neuronal loss in the DRG from patients with painful diabetic peripheral neurop-athy.[19] Transcriptional responses vary substantially across different nerve insults,[44] so it would be of interest to test whether neuronal loss and the subpopulation vulnerability reported in this study are common features across different types of insults.

Using multiple approaches, we assess the naïve mouse L4 DRG to contain approximately 8000 neurons, consistent with a previous estimate,[67] and observed a frank loss of small-diameter neurons following injury. However, the extent of loss observed using our semiautomated approach was less than that observed using manual techniques.[67] Two major limitations in this study may explain this discrepancy: First, owing to technical issues, the cleared DRG dataset is unpaired ipsilateral–contra-lateral which adds larger variability. Second, the analysis method is prone to undercounting deep nuclei. The signal-to-noise is better for superficial nuclei and smaller tissue volumes. Given the reduction in DRG volume after SNI$_{trans}$, nuclei in larger contralateral DRG may be undercounted.

While we made efforts to profile the loss of several molecularly discrete sensory neuron populations, we acknowledge that not all subtypes were profiled. Furthermore, recent single-cell RNA sequencing has given us a more granular appreciation of the heterogeneity of sensory neurons.[42] Future studies could leverage our experimental approach and new transgenic lines to characterize the loss of neurons in more detail. Such experiments may be pertinent before embarking on molecular or functional profiling of populations post–nerve injury.

4.5. Conclusions

In sum, we have provided data from multiple complementary experimental approaches to support the hypothesis that DRG neurons are lost following nerve injury in mice. We describe a substantial loss, which is biased towards specific subpopula-tions and particularly present in small-diameter nonpeptidergic nociceptive neurons.

Conflict of interest statement

Acknowledgments

Supplemental digital content

Supplemental digital content associated with this article can be found online at http://links.lww.com/PAIN/C84.

Supplemental video content

Video content associated with this article can be found on the PAIN Web site.

References

[1] Abraira VE, Kuehn ED, Chirila AM, Springel MW, Toliver AA, Zimmerman AL, Orefice LL, Boyle KA, Bai L, Song BJ, Bashista KA, O'Neill TG, Zhuo J, Tsan C, Hoynoski J, Rutlin M, Kus L, Niederkofler V, Watanabe M, Dymecki SM, Nelson SB, Heintz N, Hughes DI, Ginty DD. The cellular and synaptic architecture of the mechanosensory dorsal horn. Cell 2017;168: 295–310.e19.

[2] Bailey AL, Ribeiro-Da-Silva A. Transient loss of terminals from non-peptidergic nociceptive fibers in the substantia gelatinosa of spinal cord following chronic constriction injury of the sciatic nerve. Neuroscience 2006;138:675–90.

[3] Barry AM, Zhao N, Yang X, Bennett DL, Baskozos G. Deep RNA-seq of male and female murine sensory neuron subtypes after nerve injury. PAIN 2023;164:2196–215.

[4] Bell AM, Utting C, Dickie AC, Kucharczyk MW, Quillet R, Gutierrez-Mecinas M, Razlan ANB, Cooper AH, Lan Y, Hachisuka J, Weir GA, Bannister K, Watanabe M, Kania A, Hoon MA, Macaulay IC, Denk F, Todd AJ. Deep sequencing of Phox2a nuclei reveals five classes of anterolateral system neurons. bioRxiv 2023.2023.08.20.553715.

[5] Bennett DL, Michael GJ, Ramachandran N, Munson JB, Averill S, Yan Q, McMahon SB, Priestley JV. A distinct subgroup of small DRG cells express GDNF receptor components and GDNF is protective for these neurons after nerve injury. J Neurosci 1998;18:3059–72.

[6] Bondok AA, Sansone FM. Retrograde and transganglionic degeneration of sensory neurons after a peripheral nerve lesion at birth. Exp Neurol 1984;86:322–30.

[7] Boucher TJ, Okuse K, Bennett DLH, Munson JB, Wood JN, McMahon SB. Potent analgesic effects of GDNF in neuropathic pain states. Science 2000;290:124–7.

[8] Bradbury EJ, Burnstock G, McMahon SB. The expression of P2X3 purinoreceptors in sensory neurons: effects of axotomy and glial-derived neurotrophic factor. Mol Cell Neurosci 1998;12:256–68.

[9] Bráz JM, Basbaum AI. Triggering genetically-expressed transneuronal tracers by peripheral axotomy reveals convergent and segregated sensory neuron-spinal cord connectivity. Neuroscience 2009;163: 1220–32.

[10] Cobos EJ, Nickerson CA, Gao F, Chandran V, Bravo-Caparrós I, González-Cano R, Riva P, Andrews NA, Latremoliere A, Seehus CR, Perazzoli G, Nieto FR, Joller N, Painter MW, Ma CHE, Omura T, Chesler EJ, Geschwind DH, Coppola G, Rangachari M, Woolf CJ, Costigan M. Mechanistic differences in neuropathic pain modalities revealed by correlating behavior with global expression profiling. Cell Rep 2018;22: 1301–12.

[11] Coggeshall RE. A consideration of neural counting methods. Trends Neurosci 1992;15:9–13.

[12] Decosterd I, Woolf CJ. Spared nerve injury: an animal model of persistent peripheral neuropathic pain. PAIN 2000;87:149–58.

[13] Denk F, Ramer LM, Erskine ELKS, Nassar MA, Bogdanov Y, Signore M, Wood JN, McMahon SB, Ramer MS. Tamoxifen induces cellular stress in the nervous system by inhibiting cholesterol synthesis. Acta Neuropathol Commun 2015;3:74.

[14] Dobin A, Davis CA, Schlesinger F, Drenkow J, Zaleski C, Jha S, Batut P, Chaisson M, Gingeras TR. STAR: ultrafast universal RNA-seq aligner. Bioinformatics 2013;29:15–21.

[15] Faul F, Erdfelder E, Lang AG, Buchner A. G*Power 3: a flexible statistical power analysis program for the social, behavioral, and biomedical sciences. Behav Res Methods 2007;39:175–91.

[16] Feng G, Mellor RH, Bernstein M, Keller-Peck C, Nguyen QT, Wallace M, Nerbonne JM, Lichtman JW, Sanes JR. Imaging neuronal subsets in transgenic mice expressing multiple spectral variants of GFP. Neuron 2000;28:41–51.

[17] Gangadharan V, Zheng H, Taberner FJ, Landry J, Nees TA, Pistolic J, Agarwal N, Männich D, Benes V, Helmstaedter M, Ommer B, Lechner SG, Kuner T, Kuner R. Neuropathic pain caused by miswiring and abnormal end organ targeting. Nature 2022;606:137–45.

[18] Guillery RW. On counting and counting errors. J Comp Neurol 2002;447: 1–7.

[19] Hall BE, Macdonald E, Cassidy M, Yun S, Sapio MR, Ray P, Doty M, Nara P, Burton MD, Shiers S, Ray-Chaudhury A, Mannes AJ, Price TJ, Iadarola MJ, Kulkarni AB. Transcriptomic analysis of human sensory neurons in painful diabetic neuropathy reveals inflammation and neuronal loss. Sci Rep 2022;12:4729.

[20] Haroutounian S, Nikolajsen L, Bendtsen TF, Finnerup NB, Kristensen AD, Hasselström JB, Jensen TS. Primary afferent input critical for maintaining spontaneous pain in peripheral neuropathy. PAIN 2014;155:1272–9.

[21] Hart AM, Terenghi G, Kellerth JO, Wiberg M. Sensory neuroprotection, mitochondrial preservation, and therapeutic potential of n-acetyl-cysteine after nerve injury. Neuroscience 2004;125:91–101.

[22] Hart AM, Wiberg M, Youle M, Terenghi G. Systemic acetyl-l-carnitine eliminates sensory neuronal loss after peripheral axotomy: a new clinical approach in the management of peripheral nerve trauma. Exp Brain Res 2002;145:182–9.

[23] Hu G, Huang K, Hu Y, Du G, Xue Z, Zhu X, Fan G. Single-cell RNA-seq reveals distinct injury responses in different types of DRG sensory neurons. Sci Rep 2016;6:31851.

[24] Hu P, McLachlan EM. Selective reactions of cutaneous and muscle afferent neurons to peripheral nerve transection in rats. J Neurosci 2003; 23:10559–67.

[25] Hulsen T, de Vlieg J, Alkema W. BioVenn—a web application for the comparison and visualization of biological lists using area-proportional Venn diagrams. BMC Genomics 2008;9:488.

[26] King T, Vera-Portocarrero L, Gutierrez T, Vanderah TW, Dussor G, Lai J, Fields HL, Porreca F. Unmasking the tonic-aversive state in neuropathic pain. Nat Neurosci 2009;12:1364–6.

[27] Leibovich H, Buzaglo N, Tsuriel S, Peretz L, Caspi Y, Katz B, Lev S, Lichtstein D, Binshtok AM. Abnormal reinnervation of denervated areas following nerve injury facilitates neuropathic pain. Cells 2020;9:1007.

[28] Li H, Handsaker B, Wysoker A, Fennell T, Ruan J, Homer N, Marth G, Abecasis G, Durbin R; 1000 Genome Project Data Processing Subgroup. The sequence alignment/map format and SAMtools. Bioinformatics 2009;25:2078–9.

[29] Li L, Zhou XF. Pericellular Griffonia simplicifolia I isolectin B4-binding ring structures in the dorsal root ganglia following peripheral nerve injury in rats. J Comp Neurol 2001;439:259–74.

[30] Liang Z, Hore Z, Harley P, Uchenna Stanley F, Michrowska A, Dahiya M, La Russa F, Jager SE, Villa-Hernandez S, Denk F. A transcriptional toolbox for exploring peripheral neuroimmune interactions. PAIN 2020; 161:2089–106.

[31] Love MI, Huber W, Anders S. Moderated estimation of fold change and dispersion for RNA-seq data with DESeq2. Genome Biol 2014;15:550.

[32] Madisen L, Mao T, Koch H, Zhuo J, Berenyi A, Fujisawa S, Hsu YWA, Garcia AJ, Gu X, Zanella S, Kidney J, Gu H, Mao Y, Hooks BM, Boyden ES, Buzsáki G, Ramirez JM, Jones AR, Svoboda K, Han X, Turner EE, Zeng H. A toolbox of Cre-dependent optogenetic transgenic mice for light-induced activation and silencing. Nat Neurosci 2012;15:793–802.

[33] Madisen L, Zwingman TA, Sunkin SM, Oh SW, Zariwala HA, Gu H, Ng LL, Palmiter RD, Hawrylycz MJ, Jones AR, Lein ES, Zeng H. A robust and high-throughput Cre reporting and characterization system for the whole mouse brain. Nat Neurosci 2010;13:133–40.

[34] McCoy ES, Taylor-Blake B, Street SE, Pribisko AL, Zheng J, Zylka MJ. Peptidergic CGRPα primary sensory neurons encode heat and itch and tonically suppress sensitivity to cold. Neuron 2013;78:138–51.

[35] McKay Hart A, Brannstrom T, Wiberg M, Terenghi G. Primary sensory neurons and satellite cells after peripheral axotomy in the adult rat: timecourse of cell death and elimination. Exp Brain Res 2002;142:308–18.

[36] Molander C, Wang H, Rivero-Melián C, Grant G. Early decline and late restoration of spinal cord binding and transganglionic transport of isolectin B4 from Griffonia simplicifolia I after peripheral nerve transection or crush. Restor Neurol Neurosci 1996;10:123–33.

[37] Nguyen MQ, Le Pichon CE, Ryba N. Stereotyped transcriptomic transformation of somatosensory neurons in response to injury. Elife 2019;8:e49679.

[38] Oliveira ALR. Apoptosis of sensory neurons and satellite cells after sciatic nerve transection in C57BL/6J mice. Braz J Med Biol Res 2001;34: 375–80.

[39] Olson W, Abdus-Saboor I, Cui L, Burdge J, Raabe T, Ma M, Luo W. Sparse genetic tracing reveals regionally specific functional organization of mammalian nociceptors. Elife 2017;6:e29507.

[40] Plummer NW, Evsyukova IY, Robertson SD, de Marchena J, Tucker CJ, Jensen P. Expanding the power of recombinase-based labeling to uncover cellular diversity. Development 2015;142:4385–93.

[41] Prescott SA, Ratté S. Pain processing by spinal microcircuits: afferent combinatorics. Curr Opin Neurobiol 2012;22:631–9.

[42] Qi L, Iskols M, Shi D, Reddy P, Walker C, Lezgiyeva K, Voisin T, Pawlak M, Kuchroo VK, Chiu I, Ginty DD, Sharma N. A DRG genetic toolkit reveals molecular, morphological, and functional diversity of somatosensory neuron subtypes. bioRxiv 2023.2023.04.22.537932.

[43] Reid AJ, Mantovani C, Shawcross SG, Terenghi G, Wiberg M. Phenotype of distinct primary sensory afferent subpopulations and caspase-3 expression following axotomy. Histochem Cell Biol 2011;136:71–8.

[44] Renthal W, Tochitsky I, Yang L, Cheng YC, Li E, Kawaguchi R, Geschwind DH, Woolf CJ. Transcriptional reprogramming of distinct peripheral sensory neuron subtypes after axonal injury. Neuron 2020; 108:128–44.e9.

[45] Schindelin J, Arganda-Carreras I, Frise E, Kaynig V, Longair M, Pietzsch T, Preibisch S, Rueden C, Saalfeld S, Schmid B, Tinevez J-Y, White DJ, Hartenstein V, Eliceiri K, Tomancak P, Cardona A. Fiji: an open-source platform for biological-image analysis. Nat Methods 2012;9:676–82.

[46] Schmalbruch H. Loss of sensory neurons after sciatic nerve section in the rat. Anat Rec 1987;219:323–9.

[47] Schmitz C, Hof PR. Design-based stereology in neuroscience. Neuroscience 2005;130:813–31.

[48] Schulte A, Degenbeck J, Aue A, Schindehütte M, Schlott F, Schneider M, Monoranu CM, Bohnert M, Pham M, Antoniadis G, Blum R, Rittner HL. Human dorsal root ganglia after plexus injury: either preservation or loss of the multicellular unit. bioRxiv 2023.02.06.526934.

[49] Schulte A, Lohner H, Degenbeck J, Segebarth D, Rittner HL, Blum R, Aue A. Unbiased analysis of the dorsal root ganglion after peripheral nerve injury: no neuronal loss, no gliosis, but satellite glial cell plasticity. PAIN 2023;164:728–40.

[50] Shi TJS, Tandrup T, Bergman E, Xu ZQD, Ulfhake B, Hökfelt T. Effect of peripheral nerve injury on dorsal root ganglion neurons in the C57 BL/6J

mouse: marked changes both in cell numbers and neuropeptide expression. Neuroscience 2001;105:249–63.

[51] Song H, Yao E, Lin C, Gacayan R, Chen MH, Chuang PT. Functional characterization of pulmonary neuroendocrine cells in lung development, injury, and tumorigenesis. Proc Natl Acad Sci 2012;109:17531–6.

[52] Takasu K, Sakai A, Hanawa H, Shimada T, Suzuki H. Overexpression of GDNF in the uninjured DRG exerts analgesic effects on neuropathic pain following segmental spinal nerve ligation in mice. J Pain 2011;12: 1130–1139.

[53] Tandrup T, Woolf CJ, Coggeshall RE. Delayed loss of small dorsal root ganglion cells after transection of the rat sciatic nerve. J Comp Neurol 2000;422:172–80.

[54] Terenghi G, Hart A, Wiberg M. The nerve injury and the dying neurons: diagnosis and prevention. J Hand Surg Eur Vol 2011;36:730–4.

[55] Usoskin D, Furlan A, Islam S, Abdo H, Lonnerberg P, Lou D, Hjerling-Leffler J, Haeggstrom J, Kharchenko O, Kharchenko PV, Linnarsson S, Ernfors P. Unbiased classification of sensory neuron types by large-scale single-cell RNA sequencing. Nat Neurosci 2015;18:145–53.

[56] Vestergaard S, Tandrup T, Jakobsen J. Effect of permanent axotomy on number and volume of dorsal root ganglion cell bodies. J Comp Neurol 1997;388:307–12.

[57] Wall PD, Gutnick M. Properties of afferent nerve impulses originating from a neuroma. Nature 1974;248:740–43.

[58] Wang C, Gu L, Ruan Y, Geng X, Xu M, Yang N, Yu L, Jiang Y, Zhu C, Yang Y, Zhou Y, Guan X, Luo W, Liu Q, Dong X, Yu G, Lan L, Tang Z. Facilitation of MrgprD by TRP-A1 promotes neuropathic pain. FASEB J 2019;33: 1360–73.

[59] Wang H, Zylka MJ. Mrgprd-expressing polymodal nociceptive neurons innervate most known classes of substantia gelatinosa neurons. J Neurosci 2009;29:13202–9.

[60] Wang R, Guo W, Ossipov MH, Vanderah TW, Porreca F, Lai J. Glial cell line-derived neurotrophic factor normalizes neurochemical changes in injured dorsal root ganglion neurons and prevents the expression of experimental neuropathic pain. Neuroscience 2003; 121:815–24.

[61] Wang X, Archibald ML, Stevens K, Baldridge WH, Chauhan BC. Cyan fluorescent protein (CFP) expressing cells in the retina of Thy1-CFP transgenic mice before and after optic nerve injury. Neurosci Lett 2010; 468:110–4.

[62] Warwick C, Cassidy C, Hachisuka J, Wright MC, Baumbauer KM, Adelman PC, Lee KH, Smith KM, Sheahan TD, Ross SE, Koerber HR. MrgprdCre lineage neurons mediate optogenetic allodynia through an emergent polysynaptic circuit. PAIN 2021;162:2120–31.

[63] Weir GA, Middleton SJ, Clark AJ, Daniel T, Khovanov N, McMahon SB, Bennett DL. Using an engineered glutamate-gated chloride channel to silence sensory neurons and treat neuropathic pain at the source. Brain 2017;140:2570–85.

[64] Welin D, Novikova LN, Wiberg M, Kellerth JO, Novikov LN. Survival and regeneration of cutaneous and muscular afferent neurons after peripheral nerve injury in adult rats. Exp Brain Res 2008;186:315–23.

[65] West CA, Davies KA, Hart AM, Wiberg M, Williams SR, Terenghi G. Volumetric magnetic resonance imaging of dorsal root ganglia for the objective quantitative assessment of neuron death after peripheral nerve injury. Exp Neurol 2007;203:22–33.

[66] West CA, Ljungberg C, Wiberg M, Hart A. Sensory neuron death after upper limb nerve injury and protective effect of repair: clinical evaluation using volumetric magnetic resonance imaging of dorsal root ganglia. Neurosurgery 2013;73:632–40.

[67] West SJ, Bonboire D, Bennett DL. StereoMate: 3D stereological automated analysis of biological structures. bioRxiv 2020:648337.

[68] Wiberg R, Novikova LN, Kingham PJ. Evaluation of apoptotic pathways in dorsal root ganglion neurons following peripheral nerve injury. Neuroreport 2018;29:779–85.

[69] Yu X, Liu H, Hamel KA, Morvan MG, Yu S, Leff J, Guan Z, Braz JM, Basbaum AI. Dorsal root ganglion macrophages contribute to both the initiation and persistence of neuropathic pain. Nat Commun 2020;11:264.

[70] Zheng J, Lu Y, Perl ER. Inhibitory neurones of the spinal substantia gelatinosa mediate interaction of signals from primary afferents. J Physiol 2010;588:2065–75.